ELSEVIER

Journal of Wind Engineering
and Industrial Aerodynamics 81 (1999) 333–345

JOURNAL OF wind engineering AND industrial aerodynamics

Wind-tunnel and numerical modeling of flow and dispersion about several building shapes

Robert N. Meroney[a,*], Bernd M. Leitl[b], Stillianos Rafailidis[b], Michael Schatzmann[b]

[a]*Fluid Mechanics and Wind Engineering, Civil Engineering, Colorado State University, Fort Collins, CO 80523, USA*

[b]*Meteorologisches Institut, Universeitat Hamburg, Bundesstrasse 55, D-20146 Hamburg, Germany*

Abstract

The flow and dispersion of gases emitted by sources located near different building shapes separately studied in various wind tunnels were determined by the commercial prognostic model FLUENT and FLUENT/UNS using the standard k–ε, the RNG k–ε, and the Reynolds-stress RSM turbulence closure approximations. Inlet conditions and boundary conditions were specified numerically to the best information available for each fluid modelling simulation. Calculations are compared against the wind-tunnel measurements, but no special effort was made to force-fit agreement between the numerical and experimental data by post adjusting, coefficients, surface roughness, initial conditions, etc., beyond the specifications supplied by the laboratory researchers. The intent of these calculations were to determine if a relatively robust commercial CFD package using "reasonable" boundary and initial conditions could be used to simulate wind engineering situations without massaging the results interactively.

Keywords: Air pollution aerodynamics; Computational fluid dynamics; Wind-tunnel fluid modelling; CFD validation; Building aerodynamics; Numerical modelling

Nomenclature

B	breadth of structure (cross wind), L
C	concentration, M/L^3

* Corresponding author. Tel.: + 1-970-491-8574; fax: + 1-970-491-8671.
E-mail address: meroney@engr.colostate.edu (R.N. Meroney)

0167-6105/99/$ - see front matter
PII: S0167-6105(99)00028-8

C_p	pressure coefficient ($= \Delta p(\frac{1}{2}\rho U_H^2)$), dimensionless
D	depth of structure (along wind), L
H	height of structure, L
I_u	longitudinal velocity turbulent intensity, dimensionless
k, κ	turbulent kinetic energy, L^2/T^2
K	dimensionless concentration ($= CUL^2/Q$), dimensionless
L	length of line source, L
$M:P$	model to prototype length scale ratio, dimensionless
Q_{source}	source strength, M/T
u^*	friction velocity $(\tau_w/\rho)^{1/2}$, L/T
U_H	velocity at building height, L/T
U_{ref}	reference velocity, L/T
U_δ	velocity at boundary layer height, L/T
z_0	surface roughness height, L

Greek symbols

α	velocity profiles power law coefficient, dimensionless
δ	boundary layer height, L
ε	turbulent dissipation, L^2/T^3

Acronyms

CFD	computational fluid dynamics
FDM	finite difference method
FEM	finite element method
FVM	finite volume method
LES	large eddy simulation
RNG	Renormalized group theory
RSM	Reynolds stress model
k–ε	turbulent kinetic energy dissipation model

1. Introduction

Flow patterns which develop in cities around individual and/or groups of buildings govern the local dispersion of pollution about the building complex and its wake. The superposition and interactions of flow patterns associated with adjacent buildings govern the motion of pollutants in urban areas. Pollutant sources are often located adjacent to such buildings resulting in complicated pollutant patterns and local areas of high concentration. A number of prognostic and diagnostic models have been developed to predict flow and dispersion within the urban environment [1,2]. Unfortunately, the validation of such models has not always been satisfactory. For example, for a U-shaped building studied by Leitl et al. [2] five different numerical models (two prognostic models: MISKAM and FLUENT and three diagnostic models: ABS, ASMUS and DASIM) were compared with measurements. Calculated downwind and

surface concentrations vary mainly in the range 5 times bigger and 5 times smaller than the corresponding wind-tunnel results, but for some calculations the variation is a factor of 10. None of the models consistently predicted within a factor of 2.

The AIJ report [1] compared 65 sets of wind-tunnel tests with 51 cases of CFD calculations. The numerical methods included finite-element methods (FEM); finite-volume methods (FVM), and finite-difference methods (FDM). The turbulence models studied included standard k–ε, improved k–ε methods, and large-eddy simulations (LES). A variety of schemes to model the convection terms and different computational methods were used (implicit, explicit, SIMPLE, SMAC, MAC, HSMAC, etc.). Both original and commercial codes were used. Skill in predicting approach flow velocity, turbulence profiles, mean and fluctuating pressure coefficients varied widely. Primary conclusions were that:

- Only the improved k–ε models reproduced the roof-top mean pressure coefficients for the 0° wind orientation.
- None of the k–ε type models could reproduce the peak mean suction coefficients on the roof for the 45° angle orientation, i.e. no model could reproduce the conical vortices on the roof.
- A k–ε–φ turbulence model was proposed by Kawamoto which did satisfactorily reproduce mean pressure coefficients for all wind approach angles, including the development of the roof-top conical vortices.
- It did not appear that the LES model cases tested correctly simulated the approach flow turbulent profiles. But examination of pressure spectra and various correlations suggested that when the flow pattern is correctly simulated, LES can estimate pressure fluctuations for the 0° wind angle.
- For the 45° wind angle the convection of fluctuating pressure along the suction area was not simulated by the LES computations.

This paper extends the general CFD validation exercise for air-pollution aerodynamics to four additional sets of wind-tunnel data. The comparison is limited to the commercial codes FLUENT and FLUENT/UNS, but it does examine the variations associated with structural versus unstructured grids and the performance of three turbulence models: the standard k–ε, the RNG k–ε, and the Reynolds-stress RSM turbulence closure approximations.

2. Wind tunnel simulation of flow about four basic building shapes (a two-dimensional street canyon, two rectangular prisms, and a cubical building)

Four sets of wind-tunnel data representing recent measurements of flow around bluff generic shape model buildings in simulated atmospheric shear layers were selected for comparison. These included a two-dimensional urban street canyon, two rectangular prismatic shapes, and a cubical building [1,3–6]. Table 1 summarizes general test characteristics.

The data sets were selected to specifically provide situations with well-documented approach flows. Inflow data included high resolution, repeated measurements of velocity, turbulence intensities, integral scales, and spectra. With the models in place

Table 1
Wind tunnel test characteristics

Test series	Model size (mm) $B:D:H$	Scale ratio $M:P$	δ model (mm)	Z_0 model (mm)	Power law coef. α	U_δ model (m/s)	I_u (%)	X-turb scale model (mm)	u^*/U_δ	k model (m^2/s^2)	ε model (m^2/s^3)
CANYON	60 : 60	1 : 500	450	1.5	0.20	1.5	20	180	0.064	0.135	0.045
CEDVAL	150 : 100 : 126	1 : 200	500	0.7	0.21	6.0	25	200	0.064	0.628	0.578
AIJ	200 : 200 : 100	1 : 60–100	—	0.15–0.25	0.19	20	20	250	—	0.050	0.005
CSU CUBE	50 : 50 : 50	1 : 2000	300	0.075	0.19	0.45	15.2	67	0.05	0.007	0.0008

Note. Street canyon is also 60 mm wide followed by another downwind building model 60 : 60 mm.

meticulous measurements of wind flow, wake characteristics, pressures, and concentrations were determined.

The CANYON model studied in the Blasius Wind Tunnel, University of Hamburg, represents a 1 : 500 scale model of a parallel row of houses with $D : H$ of a 40 : 40 m size, immersed in a power-law exponent 0.20 profile turbulent shear layer and a 0.75 m field scale surface roughness [3,4]. The canyon extended the width of the tunnel, but included end plates to separate the local flow from any wind tunnel wall effects. A line source of a tracer gas was released at mid-canyon ground level to represent the pollution introduced by street-level automobile traffic. Source velocities were set low to reduce disturbance to the canyon flow field.

The CEDVAL rectangular prism model studied in the Blasius Wind Tunnel, University of Hamburg, represented a 1 : 200 scale model with $B : D : H$ of a 30 : 20 : 25 m size, immersed in a power-law exponent 0.21 profile turbulent shear layer. Inlet turbulence quantities of turbulent kinetic energy, k, and dissipation, ε, were estimated from measurements of velocity component turbulence profiles. Tracer gases were released from four small sources distributed over the width of the model along the bottom rear face of the building near ground level.

The AIJ rectangular prism case includes data from several independent laboratories studied at several model scales varying by a factor of two. The basic model aspect ratio had a $B : D : H$ of 1 : 1 : 0.5, and was immersed in a power-law exponent profile 0.25 turbulent shear layer. Approach flow turbulent intensities varied from 0.16 to 0.26 at the height of the model.

The CSU CUBE building model chosen for numerical simulation was a plexiglass cube with $B : D : H$ of 50 : 50 : 50 mm submerged in a 1 : 2000 scale model boundary layer [6]. The turbulent shear layer had a power-law exponent 0.19 profile mean velocity. Three sources of tracer were released from the roof centerline at $\frac{1}{6}$th of the depth from the front edge, roof center, and $\frac{1}{6}$th of the depth from the rear edge.

Comparisons of numerical results to experimental data include location of primary separation, reattachment, and vortex features, concentration magnitudes, and surface pressure distributions. Reproduction of concentration distributions is a particularly difficult test for any model, since scalar dilution requires correct simulation of entrainment over the entire trajectory of each fluid parcel.

3. Numerical simulation of flow and dispersion about four basic building shapes

Version 4.4.8 of the FLUENT code as well as Version 4.2.8 of the FLUENT/UNS unstructured grid code were used for numerical simulations. The code was run on a Pentium Pro 400 MHz PC using a Microsoft NT 4.0 operating system. Calculation fields were prepared with both structured and unstructured grid generation. Various calculation domains were chosen, depending on the validation case; however, for this paper only wind directions normal to a principal building face are reported, and planes of symmetry were utilized through the longitudinal building center. Outlet and velocity inlet or symmetry boundaries were specified at the sides and top of the grid volume, while appropriate surface roughness were specified at the ground and all the

building surfaces were assumed smooth. The inflow boundary conditions were chosen to match the velocity and turbulence profiles measured during the wind-tunnel experiments. Outflow boundary conditions were chosen to maintain constant longitudinal rate of change of all dependent variables (i.e. constant slope).

Three separate turbulence models were examined for each body shape: the standard k–ε, the RNG k–ε, and the Reynolds-stress turbulence closure approximations. Default coefficients suggested by Fluent were used for all adjustable constants. Table 2 provides a summary of test cases considered for each building shape. Cases considered include a fixed-size structured grid and an adapted unstructured grid; standard k–ε, renormalized group theory k–ε (RNG), and Reynolds stress (RSM) turbulence models; inlet velocity profile; inlet k and ε values (profiles or constant as available);

Numerical simulations of CANYON are all two-dimensional calculations. All other cases have three-dimensional grids.

4. Results of validation exercise

4.1. CANYON validation

Numerical calculations produced by the k–ε and RMS turbulence models reproduced the low-velocity clockwise flow field found during wind tunnel measurements. Separation and re-circulation over the front building roof occurred for all cases. Wind speeds in the canyon were of the same order seen during the experiments. Strangely the RNG model calculations produced a counter-clockwise flow field normally only seen in narrower street canyons. Comparisons were made of the concentrations found on the interior walls of the street canyon resulting from the center-ground level line source release. As noted in Fig. 1 calculated maximum concentrations ($K = CU_{\mathrm{ref}}HL/Q_{\mathrm{source}}$) consistently over-predicted the surface concentrations by 4–6 times. Apparently, the numerical velocity and turbulence fields were more convective and less diffusive than the wind-tunnel situation.

4.2. CEDVAL validation

The limited cell structured-grid calculations did not produce a roof-top separation and recirculation flow for any turbulence model. However, for an adapted grid with greater cell density at roof-top, the anticipated roof circulation appeared. The doubly-adapted unstructured grid with an RMS model produced very realistic roof-top flows. Fig. 2 compares the resultant calculated location of flow structures about the three-dimensionsal CEDVAL block against wind-tunnel measurements. The upwind horse-shoe vortex, upwind face stagnation location, and roof-top vortex were reproduced almost exactly. But the wake cavity calculated was significantly longer and wider than that measured. This subsequently affected the distribution of calculated concentrations on the building surface.

Fig. 3 compares the calculated centerline back-face concentrations found on the CEDVAL building ($K = CU_{\mathrm{ref}}H2/Q_{\mathrm{source}}$) with wind-tunnel results. Unfortunately,

Table 2
Numerical comparison conditions

Test series	Model domain	Initial cell distribution[a,b]	Total initial live cells[a]	Adapted live cells[a]	Inlet profile specified[c]	Inlet turb specified[c]	Number and type source	Structured and adapted grids	k–ε RMS	RNG	Total cases run
CANYON	$5H:20H$	50 : 200	9,304	12,682	PL	C	1 line	Yes	Yes	Yes	6
CEDVAL	$7H:15H:4H$	36 : 20 : 60	16,644	25,218	PL	POLY	1 area	Yes	Yes	Yes	6
				52,883[d]	PL	POLY	1 area	Yes	Yes	Yes	6
AIJ	$10H:20H:5H$	25 : 100 : 25	51,592	67,293	PL	C	none	Yes	Yes	No	4
CSU CUBE	$10H:20H:6H$	25 : 100 : 30	68,004	94,840	PL	C	3 point areas	Yes	Yes	No	4

[a] For 3D cases the dimensions and cells are for symmetric domain.
[b] Cells include count for walls, inlet, outlet and symmetry planes.
[c] PL = piecewise linear profile, POLY = polynomial profile, C = constant value.
[d] Second adaptation applied.

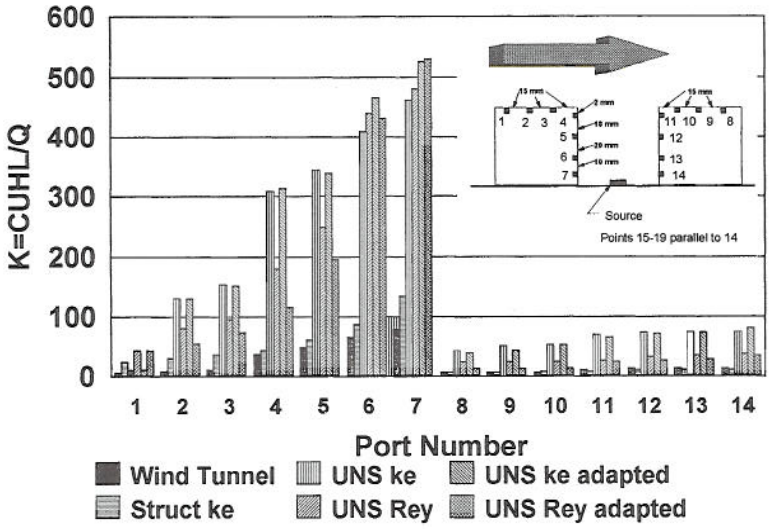

Fig. 1. Street concentrations, $K = c\,U_{\mathrm{H}}HL/Q_{\mathrm{source}}$.

Location of flow structures around the model building

Position	Wind Tunnel Measurements X	Y	Z	Numerical Model Adapted -UNS-Rey X	Y	Z
A	-0.78 H	+0.14 H	+0.00 H	-0.75 H	+ 0.12 H	+0.00 H
B	-0.40 H	+0.69 H	+0.00 H	-0.40 H	+0.65 H	+0.00 H
C	-0.09 H	+1.07 H	+0.00 H	-0.10 H	+1.08 H	+0.00 H
D	+0.88 H	+0.84 H	+0.00 H	+2.20 H	+1.00 H	+0.00 H
E	+1.78 H	+0.00 H	+0.00 H	+4.50 H	+0.00 H	+0.00 H
F	-0.13 H	+0.28 H	+0.65 H	-0.12 H	+0.28 H	+0.68 H
G	+0.72 H	+0.28 H	+0.43 H	+2.00 H	+0.28 H	+0.77 H
H	+1.68 H	+0.28 H	+0.00 H	+3.77 H	+0.28 H	+0.00 H

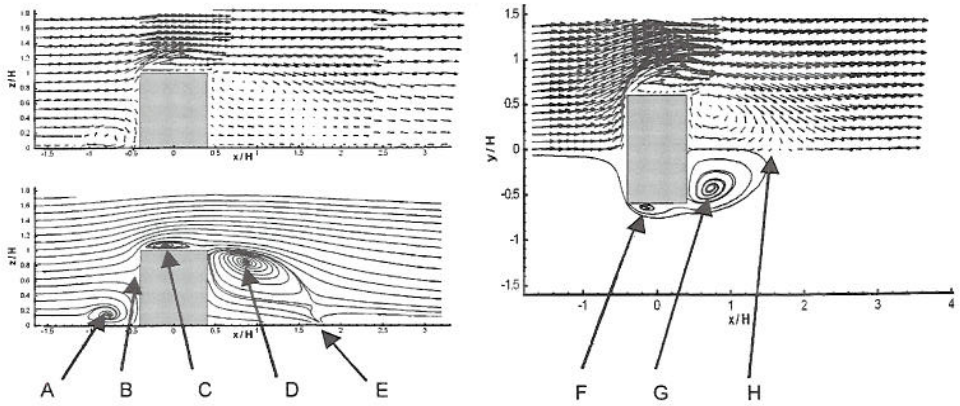

Fig. 2. Back face surface concentration on CEDVAL building $K = CU_{\mathrm{H}}HL/Q_{\mathrm{source}}$.

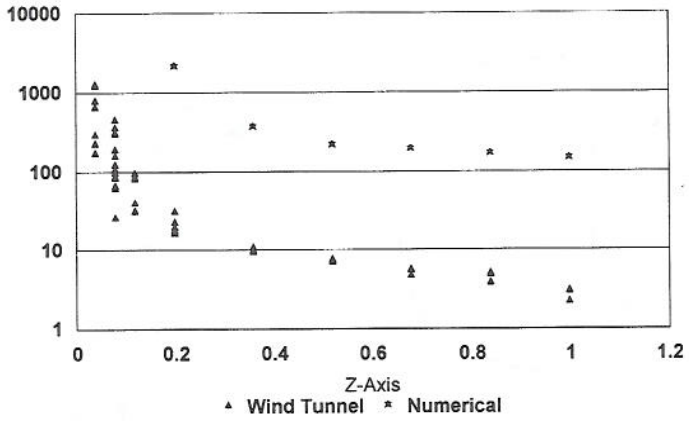

Fig. 3. Location of flow structures about model CEDVAL building.

the calculated values are consistently larger by more than an order-of-magnitude. The rate of decay of concentrations and their general distribution over the building and in the wake are reproduced. Again the calculated flow field appears to be more convective and/or less diffusive than the wind-tunnel situation.

4.3. AIJ validation

Calculations were performed for both uniform and shear velocity approach conditions to compare with equivalent wind-tunnel measurements.

4.3.1. Uniform velocity approach flow

The limited cell structured-grid calculations did not produce a roof-top separation and recirculation flow region for any turbulence model. But the adapted grid did produce such circulations, yet they did not reattach to the roof as observed. Pressure distributions were similar to those measured, but building surface pressures deviated from those measured slightly on the roof suction region. Maximum calculated roof-top pressure coefficients, C_p, were about -1.15, whereas measured values peaked at about -0.9.

4.3.2. $\frac{1}{4}$ Power sheared velocity approach flow

Strangely, neither structured nor adapted grids studied combined with any turbulence model produced roof-top separation and recirculation flow over the building model roof. Figs. 4–6 compare front, back and roof-top pressure coefficients with values measured in the presence of a $\frac{1}{4}$ power law inlet velocity profile. Despite the absence of the anticipated roof-top recirculation zones, the C_p values calculated are quite good. Maximum calculated front, back and roof-top pressure coefficients, C_p, were about 0.7, 0.25, and -1.33; whereas, measured values were 0.8, 0.25 and -1.2, respectively.

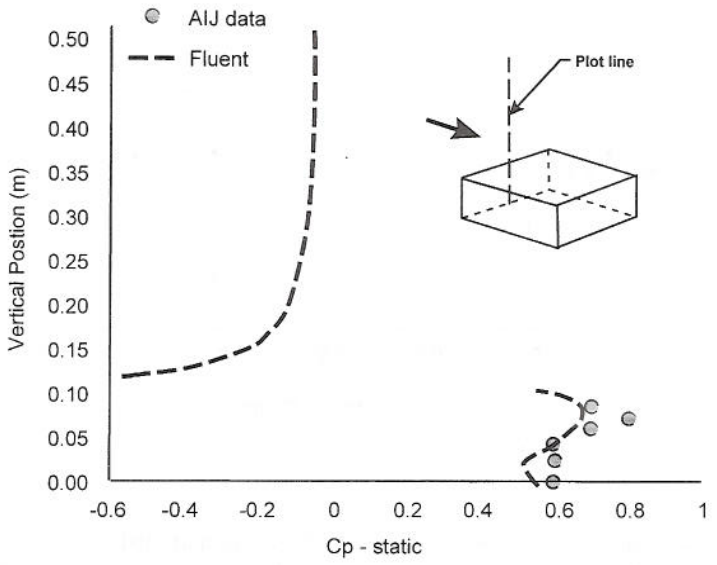

Fig. 4. Centerline front face pressure coefficients of AIJ model building, $C_p = \Delta p/(\frac{1}{2}\rho U_H^2)$.

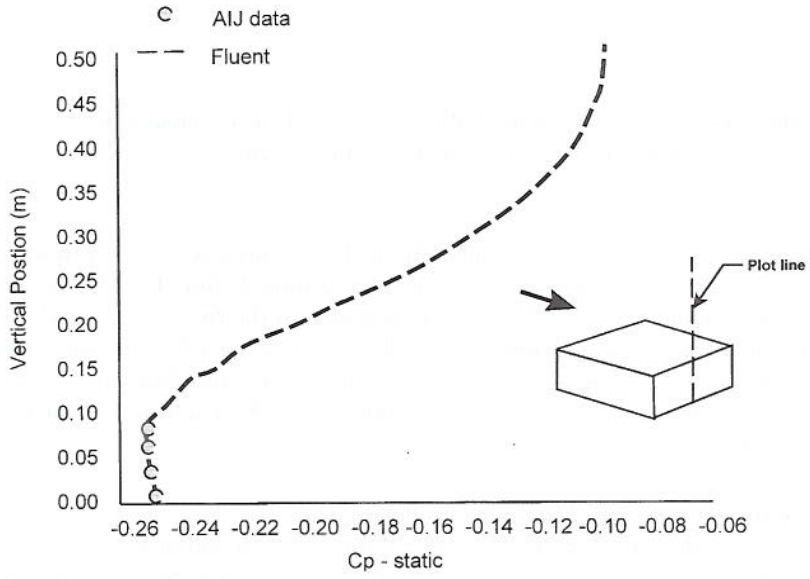

Fig. 5. Centerline back face pressure coefficients of AIJ model building, $C_p = \Delta p/(\frac{1}{2}\rho U_H^2)$.

4.4. CSU CUBE validation

Numerical calculations for both structured and adapted grids and all turbulence models tested failed to produce a recirculation zone over the upwind roof-top region.

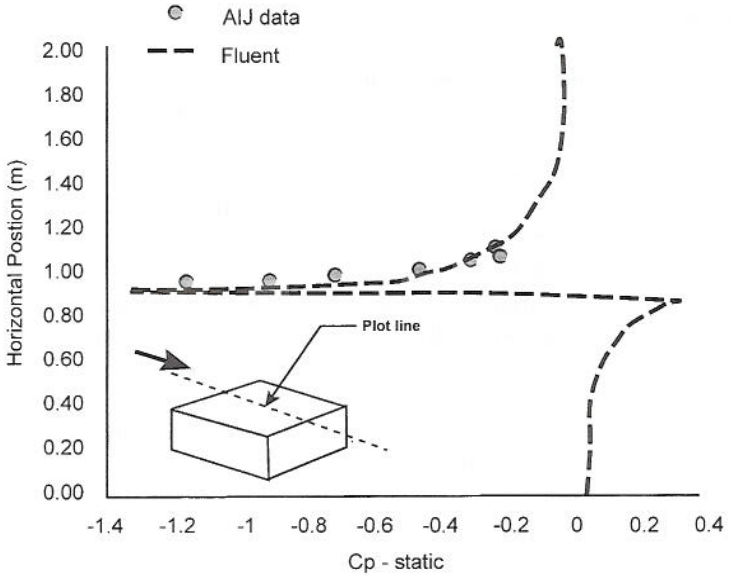

Fig. 6. Centerline rooftop pressure coefficients of AIJ model building, $C_p = \Delta p/(\frac{1}{2}\rho U_H^2)$.

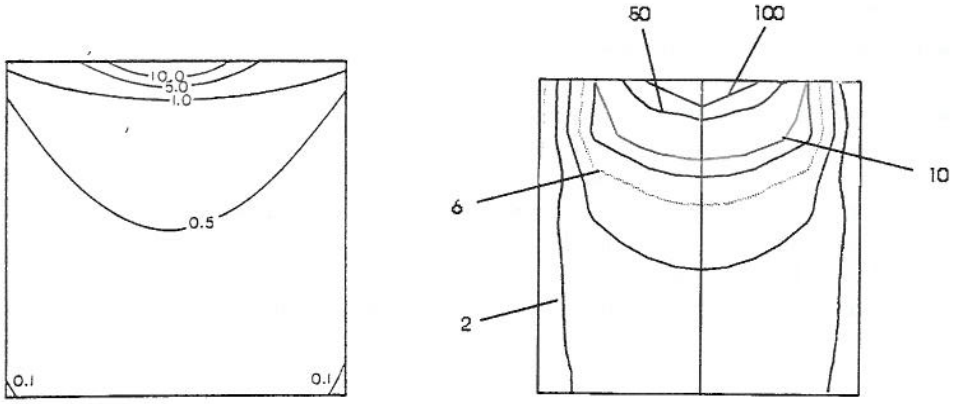

Fig. 7. Concentration isopleths on top, side and back faces of CSU CUBE model, $K = CU_{ref}H^2/Q_{source}$. Source release location on rooftop $\frac{5}{6}$ H from front edge.

Hence, plumes released on the roof front and center were not convected upwind as observed in the wind tunnel. In addition, concentrations predicted were consistently larger than those measured. Concentration patterns were reproduced, but magnitudes were frequently an order-of-magnitude too large. Fig. 7 compares concentration isopleths on the down-wind faces of the cubical model. Note that contour shapes are preserved, but magnitudes differ.

5. Conclusions

Wind-tunnel flow visualization tests performed during the CSU CUBE experiments demonstrated that a recirculation cell should exist over the front roof-top. In addition, visualization demonstrated that flow circulations are definitely intermittent – that is separation and recirculation regions develop, wash away resulting in uniformly down-wind flows over the roof, and then the circulation zone redevelops. Yet for a Reynolds-averaged type numerical model, such intermittency can not be replicated. The intermittent nature of bluff-body flows explains why numerical calculations consistently over-predict surface concentrations downwind of the source locations. These same intermittent periods of flow development partially explain the differences observed between the calculated and measured concentrations for the CANYON, CEDVAL and CUBE models.

Numerical prediction of pressure patterns were quite realistic, magnitudes were close enough to permit realistic engineering calculations, even when flow details were not replicated. This suggests that mean pressure fields are less sensitive to numerical model details than other validation criteria.

Summarizing the results of this comparison exercise with a commercial CFD code, one concludes that:

- Concentration magnitudes about sources of tracer released in the vicinity of bluff bodies are consistently over-predicted by numerical models using conventional Reynolds-averaged type turbulence models (CANYON, CEDVAL and CUBE tests).
- In some cases, different models (RNG versus k–ε and RSM) actually predicted reversal of flow for the same situation (CANYON tests).
- Upwind, side and front roof-top flow structures were replicated by numerical models, but the wake cavity was too large (CEDVAL tests).
- Mean pressure coefficients produced over the model surface were reasonably accurate, but not very sensitive to the degree of grid adaptation or turbulence model chosen.
- Typically, RSM turbulence models produced somewhat more realistic results than the k–ε or RNG models.
- Adapted grids provided a convenient way to reproduce flow details of separation and reattachment over the model surface without excessive calculation cells.

References

[1] Architectural Institute of Japan, Working group for numerical prediction of wind loading on buildings and structures, Sub-committee for wind engineering data unit for structural design, Numerical Prediction of Wind Loading on Buildings and Structures, February 1998, 74pp.

[2] B.M. Leitl, P. Kastner-Klein, M. Rau, R.N. Meroney, Concentration and flow distributions in the vicinity of U-shaped buildings: Wind-tunnel and computational data, J. Wind Eng. Ind. Aerodyn. 67&68 (1997) 745–755.

[3] R.N. Meroney, M. Pavageau, S. Rafailidis, M. Schatzmann, Study of line source characteristics for 2-D physical modelling of pollutant dispersion in street canyons, J. Wind Eng. Ind. Aerodyn. 62 (1996) 37–56.

[4] R.N. Meroney, S. Rafailidis, M. Pavageau, Dispersion in idealized street canyons, in: S.E. Gryning, F.A. Schiermeier (Eds.), Air Pollution Modeling and Its Application XI, NATO Challenges of Modern Society, Plenum Press, New York, 1996, pp. 451–458.
[5] B. Leitl, M. Schatzmann (1998), Compilation of experimental data for validation purposes, CEDVAL, Meteorology Institute, Hamburg University (Website: www.mi.uni-hamburg.de/cedval), May 1998.
[6] W.W. Li, R.N. Meroney, Gas dispersion near a cubical model building, Part I. Mean concentration measurements, J. Wind Eng. Ind. Aerodyn. 12 (1983) 15–33.